The projections of China precipitation and extreme event

Rongsheng Jiang, Ming Sun, Xiao Shi
Jiangsu Provincial Meteorological Service Center

Objectives

Previous studies have typically focused on evaluating RCMs' present climate biases and future climate changes between simulations driven by different GCMs and/or under different scenarios. However, very few have investigated connections between these biases and changes, where a systematic propagation may increase the overall projection uncertainty. Identifying these connections is important to determine projection uncertainties that are caused by model structural deficiencies. The lack of physics understanding renders it difficult to assess the signal robustness of the projected regional changes, especially for precipitation.

Therefore, this study used a state-of-the-art regional Climate-Weather Research and Forecasting model (CWRF, Liang et al. 2012) to downscale the National Center for Atmospheric Research Community Climate System Model V4.0 (CCSM4) simulations, focusing on precipitation projections in China and more importantly physics understanding of regional changes.

Methods

The lateral boundary conditions (LBCs) driving CWRF were from CCSM4 simulations in the CMIP5 archive (available from http://rda.ucar.edu/datasets/ ds316.0). This study used its historical simulation for the present climate and a projection for the future climate under the high emission scenario Representative Concentration Pathway (RCP8.5), in which the anthropogenic radiative forcing reaches 8.5 W·m^{-2} at the end of 2100 (Moss et al. 2010).

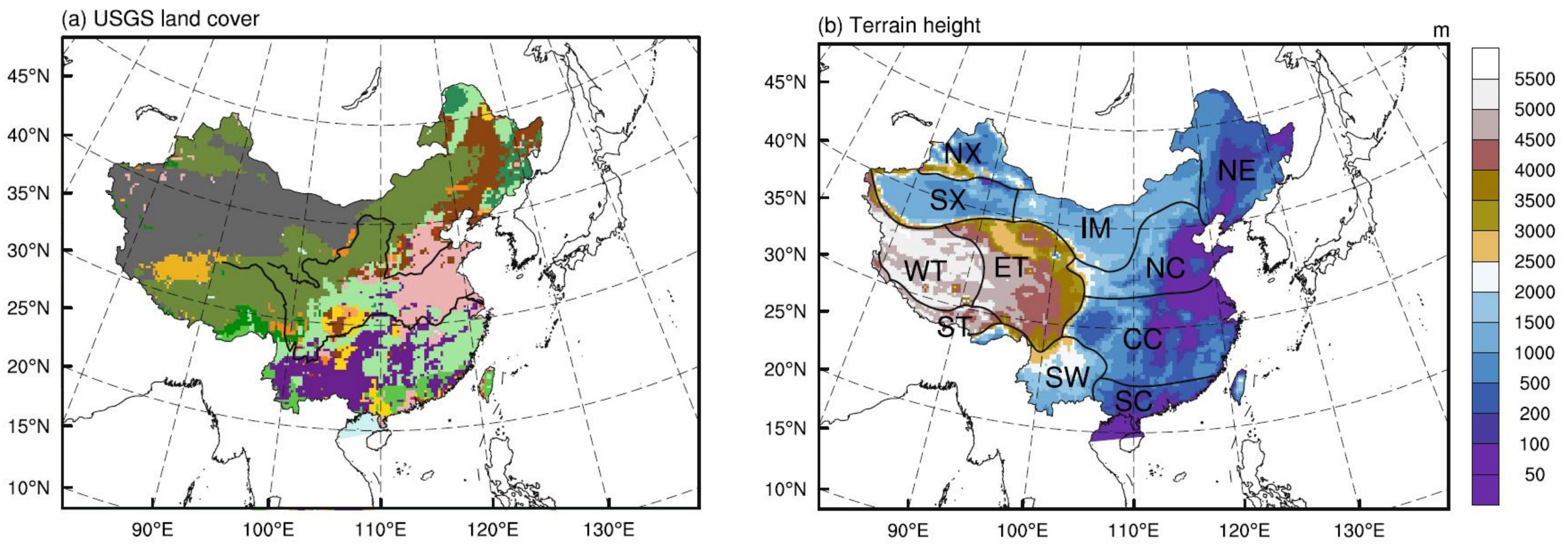

Fig. 1 The CWRF computational domain overlaid with **a** the dominant USGS land cover category and **b** the topography height and black bold lines dividing 11 major climate regimes

In additional to the typical evaluation of the climatological mean precipitation (PRA) distributions, this study elaborated the comparison of extreme precipitation characteristics.

Table 1. Precipitation characteristics used in this study

Indicator	Definition	Units
PRA	Average precipitation (daily precipitation >= 1.0 mm)	mm day^{-1}
P95	95th percentile of daily precipitation	mm day^{-1}
NRD	Count of rainy days (daily precipitation >= 1 mm)	days
CDD	Maximum number of consecutive days with daily precipitation < 1 mm	days

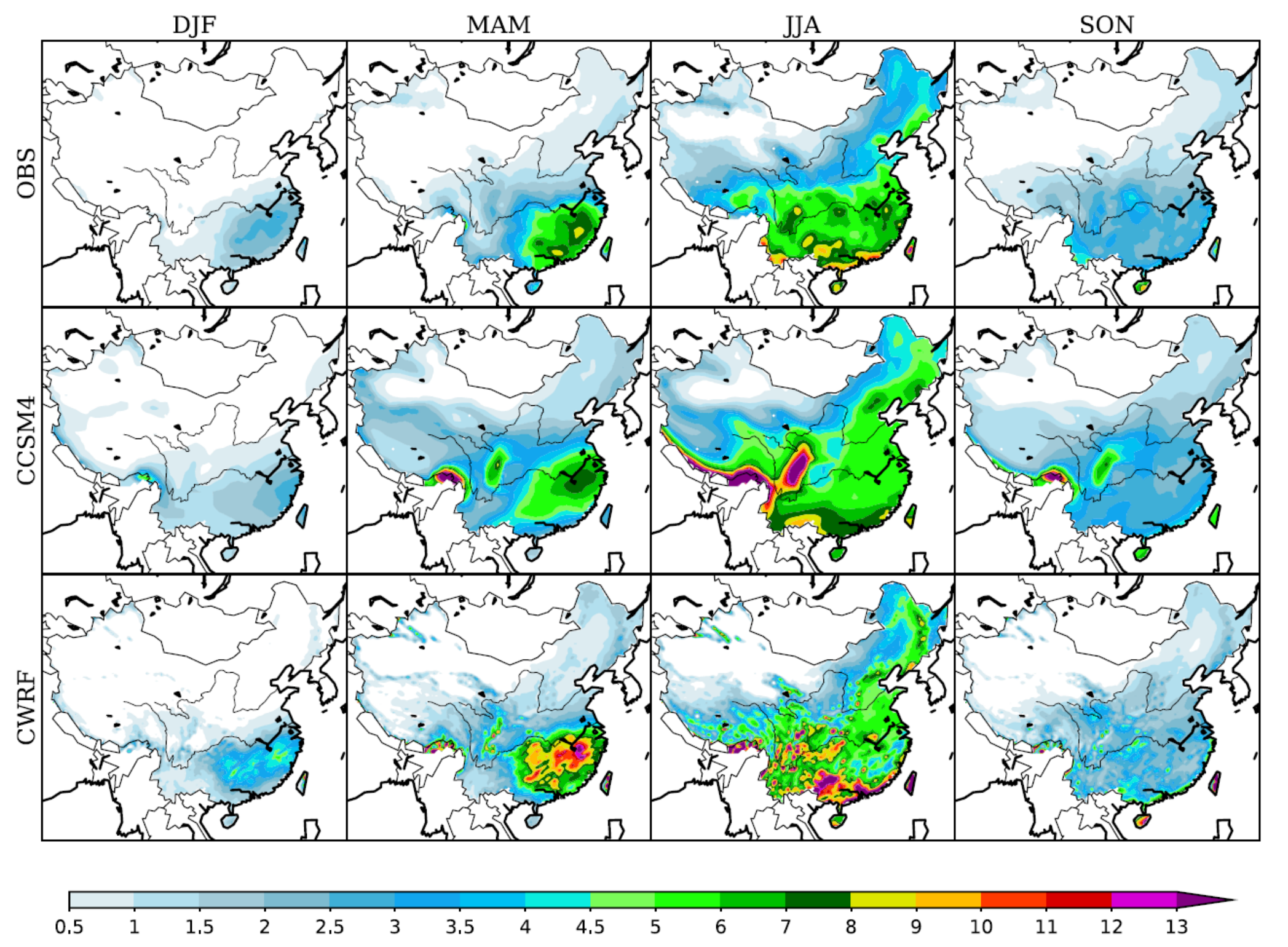

Fig. 2 Geographic distributions of seasonal mean precipitation (PRA, mm day^{-1}) observed (OBS), simulated by CCSM4, and downscaled by CWRF in winter (DJF), spring (MAM), summer (JJA) and autumn (SON) as averaged during the present (1974–2005)

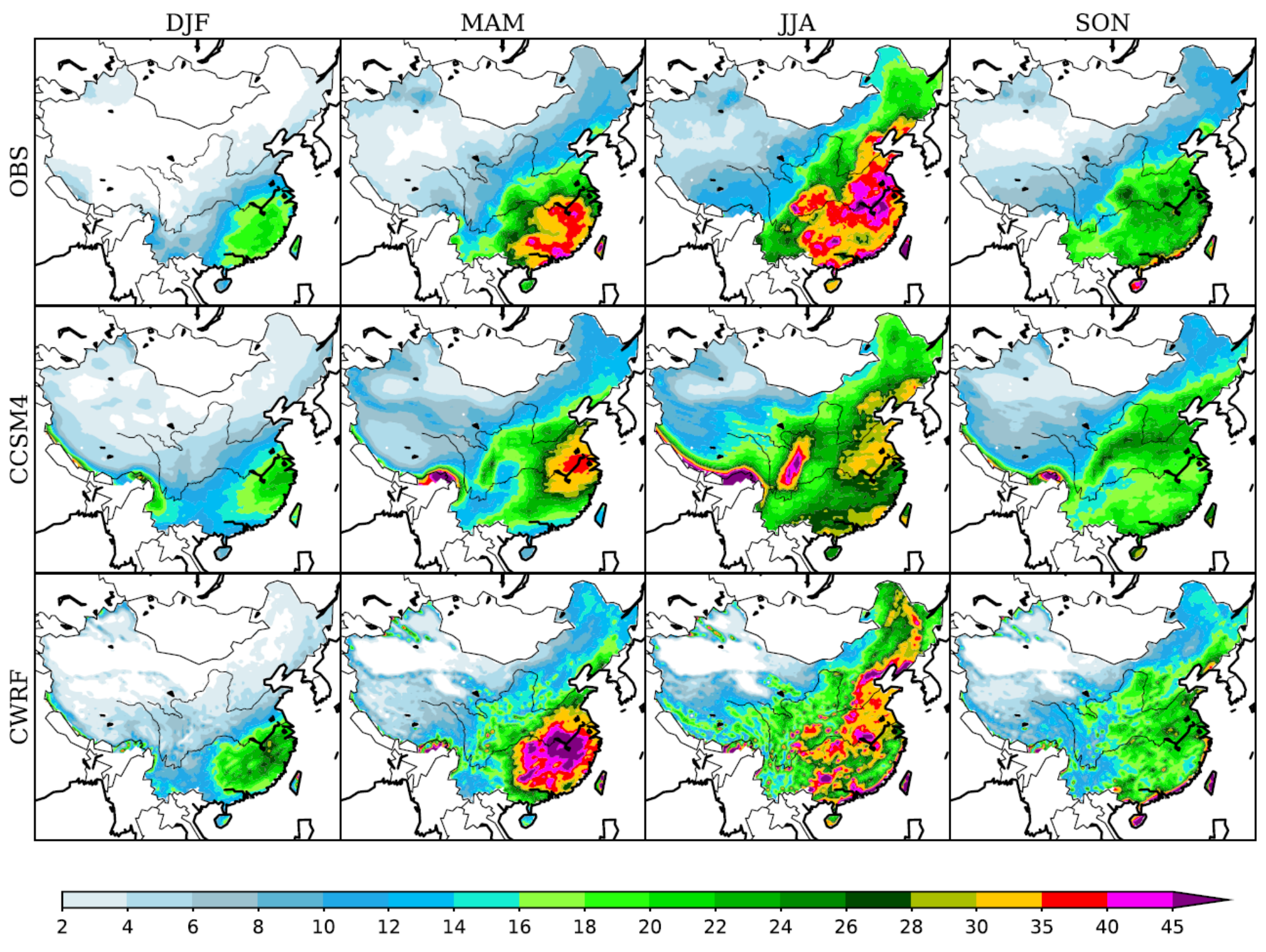

Fig. 3 Same as Fig. 2 except for the 95th percentile of daily precipitation (P95, mm day^{-1})

Results

Overall, CWRF outperformed CCSM4 in capturing mean precipitation (PRA) distribution details with a finer structure (Fig. 2, 3), smaller biases (Fig. 4), and higher correlations. CWRF improved over CCSM4 also in simulating extreme precipitation (P95) patterns for all seasons.

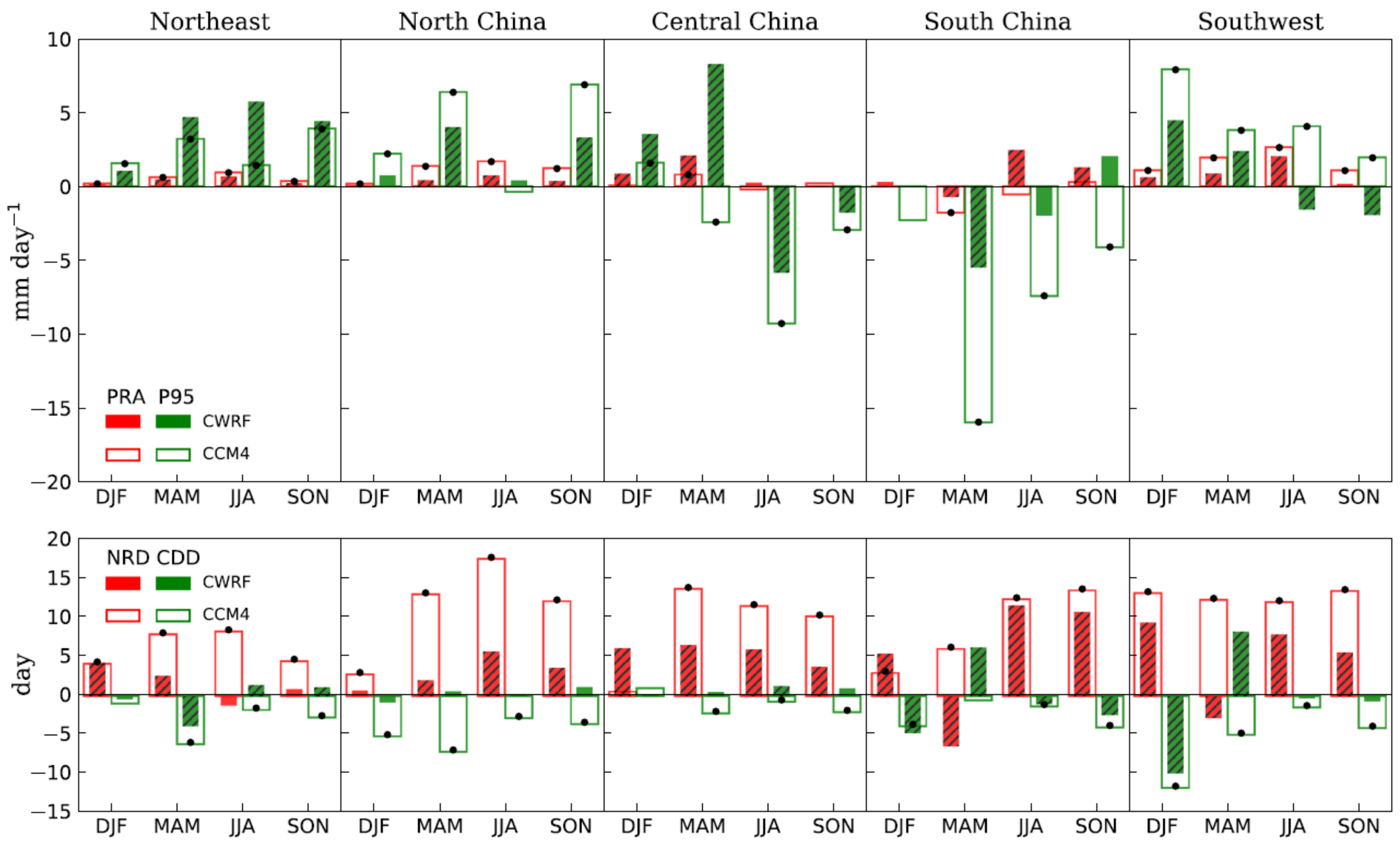

Fig. 4 Biases (from observations) of seasonal precipitation characteristics (PRA and P95 in mm day^{-1}; NRD and CDD in days) averaged over the five key regions as simulated by CCSM4 and downscaled by CWRF. Hatches and black circles denote statistically significant differences at the 90% confidence level for CWRF and CCSM4 respectively

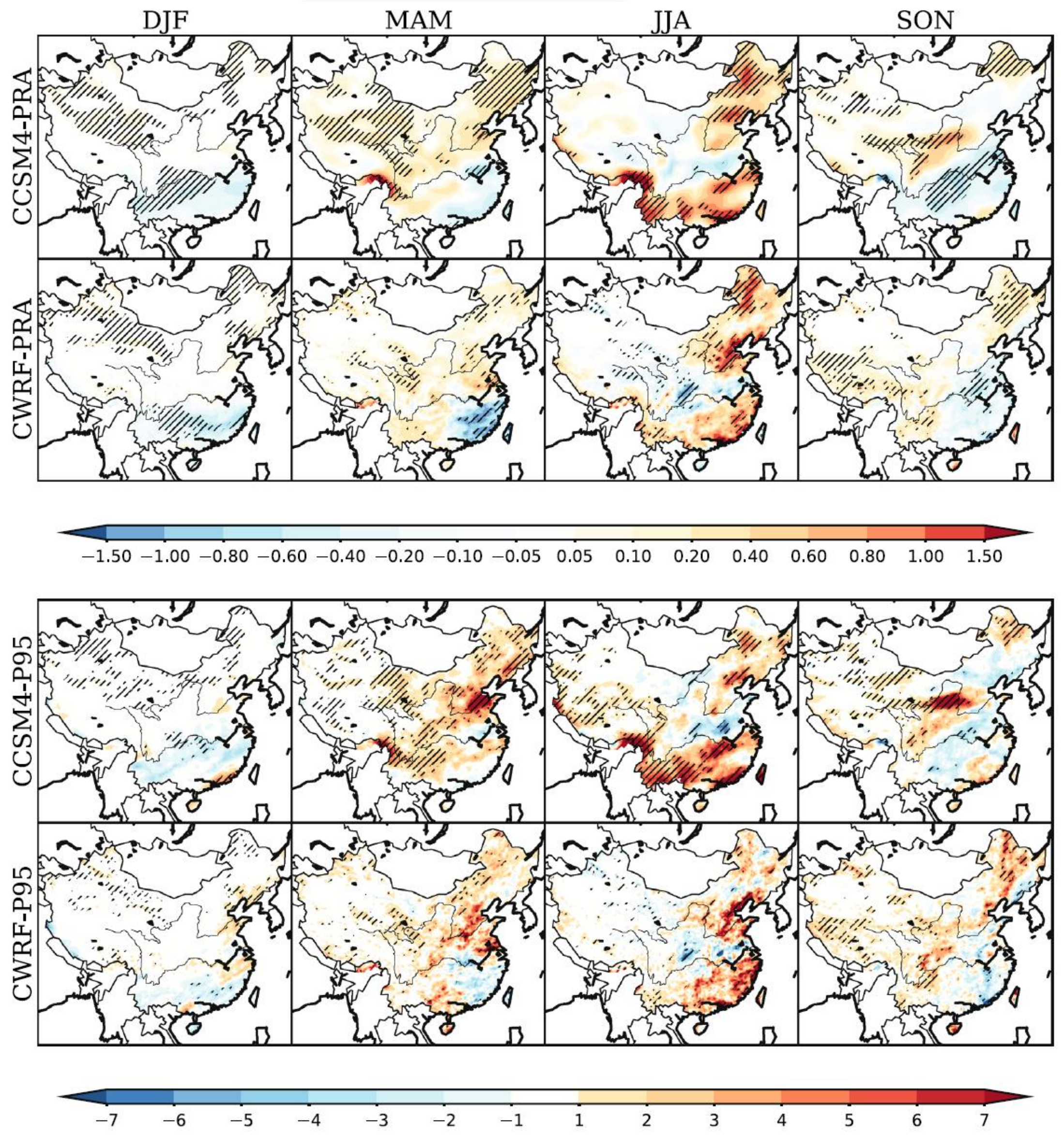

Fig. 5 Geographic distribution of seasonal mean precipitation (PRA, mm day^{-1}) and extreme precipitation (P95, mm day^{-1}) changes from the present (1974–2005) to future (2019–2050) as projected by CCSM4 and downscaled by CWRF.

Figures 5 compare the future (2019–2050 minus 1974–2005) changes in seasonal precipitation statistics (PRA, P95) as projected by CCSM4 and downscaled by CWRF.

CWRF produced significant improvements in timing, intensity, location, and coverage. However, CWRF overestimated rain intensity in South China during May–August and in Central China during April–May. Nonetheless, the overall improved ability to capture these detailed spatiotemporal variations was fundamental for CWRF to outperform CCSM4 in reproducing the observed major rainfall characteristics (seasonal mean and extremes, rainy and dry days) averaged over the distinct regions in eastern China.

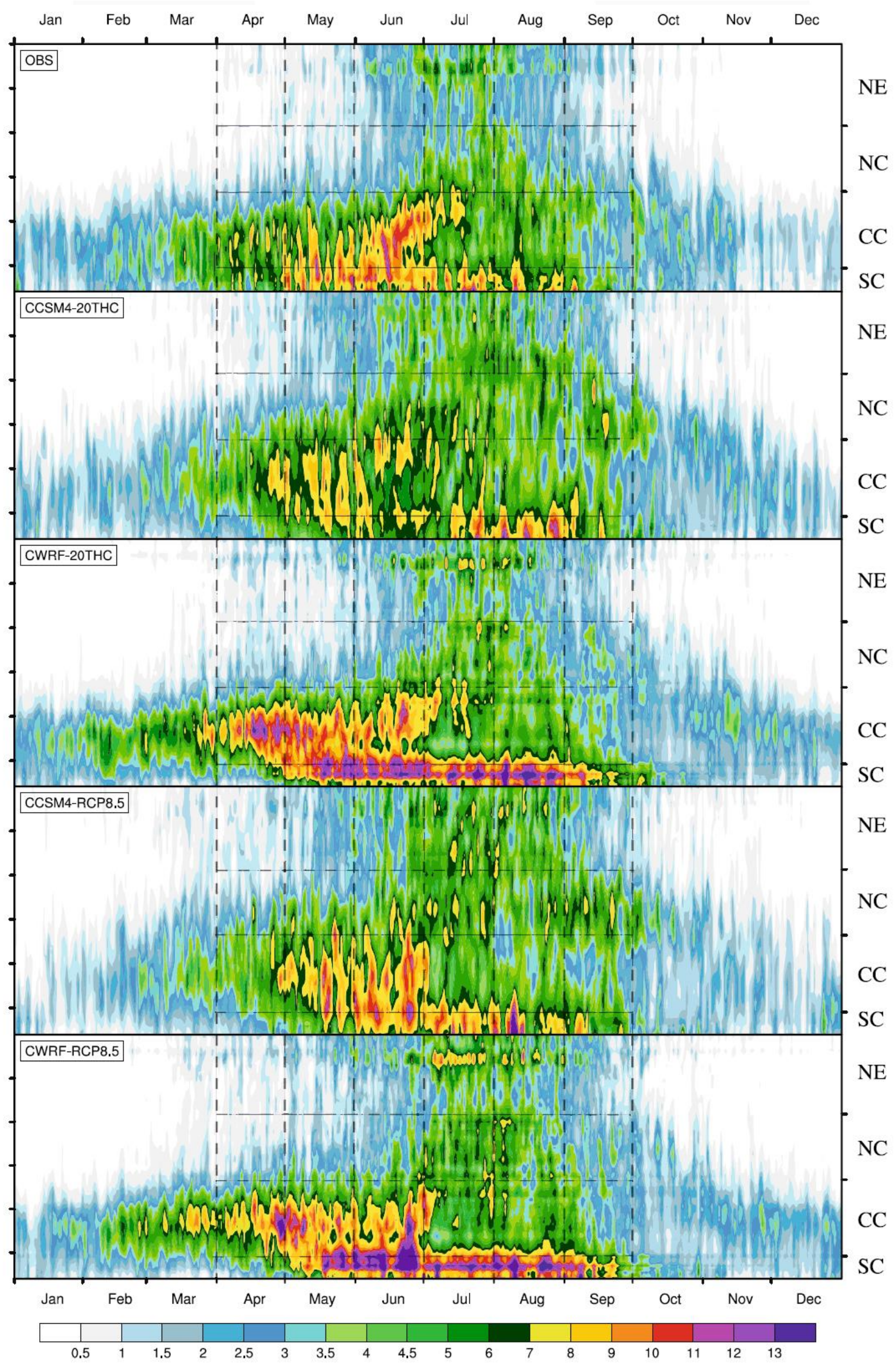

Fig. 6 Annual cycles of latitude-time cross-sections of daily precipitation (mm day^{-1}) averaged across 105–122° E as observed (OBS), simulated (20THC) and projected (RCP8.5) by CCSM4, and downscaled by CWRF